Research Article

Ameliorated Stomach Specific Floating Microspheres for Emerging Health Pathologies Using Polymeric Konjac Glucomannan-Based Domperidone

Jamal Moideen Muthu Mohamed ⓘ,[1] **Nikita Mahajan,**[2] **Mohamed El-Sherbiny** ⓘ,[3,4]
Shagufta Khan ⓘ,[2] **Rasha Hamed Al-Serwi,**[5] **Mohammed A. Attia,**[3,6]
Qamar Alsayed Altriny,[3] **and Ahmed H. Arbab** ⓘ[7]

[1]*Vaasudhara College of Pharmacy, Sante Circle, Chintamani Road, Hoskote, 562114 Karnataka, India*

[2]*Institute of Pharmaceutical Education and Research, Borgaon (Meghe), Wardha, Maharashtra 442 001, India*

[3]*Department of Basic Medical Sciences, College of Medicine, AlMaarefa University, P.O. Box 71666, Riyadh 11597, Saudi Arabia*

[4]*Department of Anatomy, Faculty of Medicine, Mansoura University, Mansoura, Egypt*

[5]*Department of Basic Medical Sciences, College of Dentistry, Princess Nourah Bint Abdulrahman University, P.O. Box 84428, Riyadh 11671, Saudi Arabia*

[6]*Department of Clinical Pharmacology, Faculty of Medicine, Mansoura University, 35516 Mansoura, Egypt*

[7]*Department of Pharmacognosy, Faculty of Pharmacy, University of Khartoum, Al-Qasr Ave, Khartoum 11111, Sudan*

Correspondence should be addressed to Shagufta Khan; shaguftakhan17@rediffmail.com
and Ahmed H. Arbab; ahmed.arbab@uofk.edu

The goal of this study was to use polymeric konjac glucomannan (KGM), Kollidon VA 64 (KVA64), and glutaraldehyde to ameliorate stomach specific floating microspheres (SSFM) using domperidone (DoN) to increase *in vivo* bioavailability and emerging health pathologies. The SSFM were made using the emulsion cross-linking process, and the polymer was chosen based on its ability to get cross-linked. The thermodynamic parameters were used to determine the A_L classes of phase solubility curves using ideal complexes produced with KVA64. The optimal interaction constants at 25 and 37°C were found to be 116.14 and 128.05 M^{-1}, respectively. The prepared SSFM had an average particle size (PS) of 163.71 ± 2.26 mm and a drug content of $96.66 \pm 0.32\%$. It can be determined from *in vitro* drug release experiments that drug release is good in terms of regulated drug release after 12 h ($92.62 \pm 2.43\%$). The SSFMs were approximately sphere-shaped and had smooth surfaces, according to the morphological data. SSFMs were investigated using Fourier transform infrared (FT-IR) spectroscopy, X-ray diffraction (XRD), and differential scanning calorimetry (DSC), and no chemical structural changes were identified. The SSFMs produces a considerable gastric residence time with optimal DoN release and absorption in stomach fluid, and the mean residence time (17.36 ± 1.4 h) and $t_{1/2}$ (10.47 ± 0.6 h) were considerably longer ($p < 0.05$) than those obtained following i.v. treatment (MRT = 8.42 ± 1.2 h; $t_{1/2} = 9.07 \pm 0.7$ h). The SSFMs maintained good physical stability for three months when stored at room temperature.

1. Introduction

Despite their potential pharmacological action, the bottleneck for the effective introduction of many new drugs is their poor solubility. Aqueous insoluble compounds account for over 90% of all chemicals in pharmaceutical drug delivery systems. Poor solubility can be a big concern since an active pharmaceutical ingredient (API) cannot reach its molecular target in the body if it remains undissolved in the gastrointestinal tract (GIT) and is therefore removed

[1]. As a result, improving the molecules solubility is a crucial step in ensuring that it survives the pharmaceutical development process. If their bioavailability is restricted by their water solubility, even compounds with a significantly positive impact on their physiological target will not be developed further. Furthermore, poorly water soluble drugs are commonly given at large doses to attain the required plasma drug concentration, resulting in increased adverse reactions and therapy costs, as well as unpredictable pharmacological responses, resulting in poor patient compliance.

Additionally, if the drug is expensive, the manufacturing cost will rise since a huge proportion of API will be used to research and produce the medicinal product. Since a result, solubilization technologies that address this issue are becoming increasingly relevant to the pharmaceutical industry, as they offer up new avenues for developing effective and marketable drug delivery systems from APIs that would otherwise be lost [2]. Solid dispersion, cocrystallization, micronization, nanonization, solid lipid nanoparticles microemulsion, self-microemulsifying and nanoemulsifying drug delivery systems, and liposomes are some of the methods used to improve the dissolution and solubility of poor aqueous soluble drugs [3].

Solid dispersions (SDs) have found more attention over the years for two main reasons: first, they afford a greater enhancement in dissolution or solubility rate associated to crystal habit ensuring effective, and second, they reduce recrystallization/agglomeration of drug molecules due to molecular interactions with the carrier matrices [4]. The SD permits high drug concentrations to be available in the GIT by increasing their apparent solubility and provide several order of improvement in bioavailability of poorly water-soluble drugs. Amorphous carriers like PVP, PEG, cross-povidone (PVP-CL), PVP-VA, and polymethacrylates are widely used to improve solubility. Meloxicam ASD was made by utilizing HPMC and carriers such as polyacrylates and polymethacrylates. SDs of meloxicam exhibited much better dissolution behavior than crystalline meloxicam. It was reported that meloxicam was presented in the amorphous form by SDs which lead to its improved dissolution behavior [5]. Prepared SDs of chlortetracycline hydrochloride using hydrophilic polymers like PVP and copovidone, Authors reported that SDs increased almost ten-fold chlortetracycline hydrochloride solubility, which they attributed to the amorphous characters of the SDs, proposing the event of intermolecular interactions.

While a drug displays not only poor aqueous solubility but also a pH-dependent solubility, it becomes imperative to retain the formulation at the site in the GIT where it shows maximum solubility in order to improve its bioavailability. For the drugs which show greater solubility in the stomach than other parts of the GIT, one of the most significant techniques of achieving stomach retention of such drugs in order to increase their bioavailability is to use a floating drug delivery device.

Entrapment of air (e.g., hollow chambers) or the integration of low-density constituents can produce the inherent low density (e.g., oils or fatty materials or foam powder). A single-unit floating system containing polypropylene foam powder, matrix-forming polymers, drug, and filler was recently presented. This device exhibited good floating behavior and accurate drug release control. Single-unit dosage formulations, on the other hand, have been associated to problems like sticking together or becoming blocked in the GIT, both of which can be unpleasant [6]. Multiple-unit floating systems, on the other hand, may be appealing since they have been shown to reduce inter- and intrasubject variability in drug absorption as well as the danger of dose spillage.

Numerous multiple-unit floating systems, such as the air compartment multiple-unit system, hollow microspheres (microballoons), microparticles designed for low-density foam powder, and low-density beads, can be widely dispersed throughout the stomach, allowing for a longer and more reliable drug release [7]. Nonetheless, to regulate their qualities, these several unit floating systems are created using tough and demanding approaches with laborious operational settings.

In this study, an attempt was made to develop floating microspheres using a simple, scalable approach that did not require the addition of an effervescent agent, low-density oil, or foam powder, all of which are crucial processing factors. Floating microspheres were prepared using natural polysaccharide konjac glucomannan (KGM) because it is nontoxic, biodegradable, and biocompatible and easily available from the tuber of the amorphophallus plant. KGM is made up of 1 : 6 molar ratio of 4-linked -D- mannose and glucose units. It is a somewhat branched polymer having acetyl groups on the backbone ninth and twentieth positions. The innate polysaccharide KGM was used to make floating microspheres since it is nontoxic, biodegradable, and biocompatible, as well as being readily accessible from the tuber of the *amorphophallus* plant. In the molar ratio of 1 : 6, KGM is made up of 1, 4-linked β-D-mannose and glucose units. It is a quite branched polymer having acetyl groups on the backbone's ninth and twentieth positions [8]. It has a great feature of quick gelling and high swelling capacity, which is helpful to the floating ability, due to the large number of hydroxyl groups on the saccharide units. However, studies on application of KGM in the preparation of floating microspheres are nonexistent.

In the present investigation, domperidone (DoN) is used as a model drug. The DoN is a peripherally selective dopamine D_2 and D_3 antagonist. By inhibiting dopamine receptors in the gastric antrum and duodenum, it promotes upper gastrointestinal motility to a partial support and lower esophageal sphincter pressure. DON has poor water solubility, which displays pH dependence with greater solubility in stomach than intestine. Its oral bioavailability is poor (13 to 17%) due to poor aqueous solubility [9]. Therefore, it was attempted to first improve the solubility of DoN by formulating ASD using Kollidon VA 64 and successively formulating floating microspheres loaded with DPASD that can be retained in the stomach.

2. Materials

Domperidone (DoN) and Kollidon VA 64 (KVA64) were received as gift samples from FDC Limited, Mumbai, India. Konjac glucomannan (KGM) was purchased from Konjac

TABLE 1: Various composition of prepared SSFMs.

SSFMs	KGM		Drug % w/w of polymer ratio		Equ. Wt. of SD (mg)
	(%w/w)	For 15 mL (mg)	% w/w	wt.in mg	
DF1	1	150	30	45	124.86
DF2	1.5	225	30	67.5	187.29
DF3	2	300	30	90	249.72
DF4	1	150	40	60	166.48
DF5	1.5	225	40	90	249.72
DF6	2	300	40	120	322.96

∗Volume of KGM solution was 15 mL, cotton seed oil was 30 mL, and glutaraldehyde (25% w/v) was 50 mL for all batches.

Food, China. Acetone, Acetonitrile and HPLC grade of methanol were procured from the Loba Chemie Pvt. Ltd., Mumbai, India. Ethanol and isopropyl alcohol were purchased from Thermo Fisher Scientific Pvt. Ltd., Mumbai, India.

2.1. Phase Solubility Study. The phase solubility investigation was carried out according to Higuchi and Connors approach [10]. Excess DoN was added to distilled water containing various concentrations of Kollidon VA 64 in 20-mL capped bottles, stirred for 48 h at 25 and 37 ± 0.5 °C on magnetic stirrer, filtered, and spectrophotometrically analyzed at 283 nm using a double-beam spectrophotometer (UV 2401(PC),S.220V Shimadzu Corporation, Japan). According to the following equation, the apparent complexation constant $K_{1:1}$ of DoN-KVA64was estimated from the intercept and slope of the straight line of the phase solubility graph.

$$K_{1:1} = \frac{Slope}{S0\,(1 - Slope)}, \tag{1}$$

where S_0 (intercept) is the solubility of DoN in the absence of complexing agent.

2.2. Preparation of SD. Solid dispersion was prepared by the solvent evaporation method [11]. DoN and KVA64 (1 : 1) were added to 10 mL solvents containing ethanol and acetone (1 : 1). The mixture was continuously stirred (100 rpm with 37 ± 1°C), and the solvent was evaporated. The mass was crushed, passed through the sieve no. 40, and stored in desiccators, and physical mixture was also prepared by geometrical mixing of drug and carrier. Drug content of SD was determined by stirring 100 mg SD in 100 mL ethanol for 24 h, and then the mixture was filtered, diluted suitably, and analyzed spectrophotometrically at 208 nm.

2.3. Saturated Solubility (SS) Study. The SS of samples (DoN, PM, and SD) was determined in distilled water and pH 1.2 at room temperature (RT). Excess amount of samples was added 20 mL of above stated solution in screw-capped glass vials. Then, the vials were stirred for 48 h at 25 ± 0.5°C using thermostatically controlled magnetic stirrer (REMI 2) retained at speed of 50 strokes per min [12]. After 48 h, the content in respective vial was withdrawn and filtered using Whatman filter paper No.42, and the amount of DoN dissolved in different medium was determined spectrophotometrically at 208 nm. Each experiment was carried out in triplicate.

2.4. Drug Content (DC). The solid dispersion (50 mg) was dispersed in 50-mL volumetric flask using ethanol and stirred for 24 h at 25 ± 0.5°C using magnetic stirrer maintained at speed of 50 strokes per min. The material was then filtered via Whatman filter paper no. 42 after 24 h [12]. The absorbance was measured at 284 nm using a twin beam UV visible spectrophotometer after appropriate dilutions were prepared.

2.5. Dissolution Study. The dissolution studies on pure DoN, PM, and SD (equivalent to 10 mg of DoN) was supported out by USP paddle apparatus (type II) by 500 mL dissolution medium (distilled water and 0.1 N HCL). Rotation speed was 100 rpm and temperature (T) was maintained 37 ± 1°C [13]. 5 mL sample was removed at regular intervals (30, 60, 90, 120, 150, 180, and 210 min), and aliquot was withdrawn and replaced with equal volume of fresh dissolution medium, filtered, and analyzed, using double-beam UV spectrophotometer at 284 nm.

2.6. Preparation of Stomach Specific Floating Microspheres (SSFM). The various concentrations of KGM were allowed to swell overnight in distilled water to get homogeneous solution, and viscosity of each solution was determined. To KGM solutions, SD equivalent to drug 30%w/w of KGM was added and emulsified with cotton seed oil, containing 0.5% w/v span 80 by homogenizing for 3 h at 3000 rpm (Table 1). Glutaraldehyde (aqueous, 25% w/v) comprising 0.5 mL of 1 N HCL was added gently to the emulsion with homogenization for 2 h, and microspheres were collected by centrifugation at 6000-8000 rpm. Thereafter, separated microspheres were washed with isopropyl alcohol to remove the excess oil from surface, and unreacted glutaraldehyde then freeze dried (Lark Innovative Fine Technology, Chennai, India, Model; Penguin Classic Plus; −20°C and 0.13 bar) for 24 h [14]. DoN content in microspheres was determined by soaking 100 mg crushed microspheres in 100 mL ethanol for 24 h and filtered and then analyzed the filtrate at 208 nm.

The following formulae were used to estimate the drug content and entrapment efficiency (EE):

$$\text{Drug Content} = \frac{\textit{Weight of drug in Microspheres}}{\textit{weight of Microsphere}},$$
$$\%\text{EE} = \frac{\textit{Actual drug content}}{\textit{Theoretical drug content}} \times 100. \tag{2}$$

2.7. Micromeritic Properties.

Particle size (PS) was determined using imaging system (Metzger optical instrument, Sr. No. 666 Mathura, India). Fifty microspheres from each batch were measured, and the average PS was determined.

For bulk density, 1 g microspheres were placed in a 10 mL capacity measuring cylinder, and volume was noted. Tapped density was determined by mentioning the volume of the known weight of microspheres after 100 taps. Moreover, micromeritic properties such as Carr's index (% compressibility), Hausner ratio, and angle of repose were evaluated according to the method described by Thapa and Chaudhary [15].

2.8. Surface Morphology.

For surface morphology, microspheres were layered with platinum and visualized under analytical scanning electron microscope (Model S-3700N, Hitachi, Japan) according to the method described by Muthu et al. [12].

2.9. Floating Study.

Microspheres (100 mg) were dispersed across the surface of a USP dissolving apparatus type II filled with 300 mL of 0.1 N HCL pH 1.2 for *in vitro* buoyancy testing. A paddle moving at 100 rpm was used to stir the medium for 12 h. Microspheres floating and settling sections were retrieved individually. The microspheres were weighed after drying, and the ratio of the mass of the microspheres that stayed floating to the overall mass of the microspheres was used to compute buoyancy percentage. The following formulas [16] were used to calculate the buoyancy percentage by dividing the mass of the microspheres that remained to float by the overall mass of the microspheres.

$$\%\text{Buoyancy} = \frac{W_f}{\left(W_f + W_s\right)} \times 100, \tag{3}$$

where W_f and W_s are the weights of the floating and settled microspheres.

2.10. Solid-State Characterization

2.10.1. Fourier Transform Infrared (FT-IR) Analysis.

FTIR analysis was performed using an FT-IR spectrophotometer (Model No. 84005 Shimadzu Asia Pacific Pvt. Ltd. Singapore). The powdered samples were pelleted with KBr, and the disc was scanned in the range of 4000-400 cm^{-1} [17].

2.10.2. Differential Scanning Calorimetric (DSC) Analysis.

For DSC, 5 mg of samples were enclosed in an aluminum pan and evaluated between 30 and 300°C at a scanning rate of 10°C.min^{-1} [17]. During the runs, a nitrogen purge at a rate of 20 mL.min^{-1} was maintained, and indium was used as a benchmark for T and heat flow calibrations (Model-DSC 60, Shimadzu Tokyo, Japan).

2.10.3. Powder X-Ray Diffraction (PXRD) Analysis.

An X-ray diffraction examination was done on a copper anode operating under CuK radiation (1.5406, 45 kV, and 40 mA) (SmartLab, Rigaku Corporation, Tokyo, Japan). Patterns were made on a 2 scale with a step width of 0.05°/s from 2 to 50° at RT [17].

2.11. In Vitro Drug Release.

Drug release from SSFMs was investigated in 0.1 N HCL at pH 1.2 for 12 h using USP type II apparatus at the stirring speed of 100 rpm. Equivalent weight of SSFMs to 10 mg of DoN was kept in 500 mL of dissolution medium continued at 37 ± 0.5°C. Throughout the dissolution study, 5 mL aliquot was withdrawn at predetermined time intervals and analyzed for percentage dissolved DoN at 283 nm. The aliquots withdrawn were replaced with equal volume of the drug-free medium [13]. Cumulative present drug dissolved was determined at each time interval and plotted against time.

2.12. Bioavailability Study in Rats

2.12.1. Experimental Design.

The study employed male Wistar albino rats weighing 200-250 g. The Institutional Animal Ethical Committee accepted the study (Approval No. IAEC/ 2018-2019). Animals were kept in polypropylene cages at T of 24 ± 2°F, with a relative humidity (RH) of 40-60% and a 12-hour light-dark cycle. The animals were under fasting for 12 h before dosing and kept fasting throughout the study and allowed to take water.

The study was conducted on 42 rats which were separated into 2 groups (21 rats in each group). Animals of group I received SSFM equivalent to 0.15 to 0.18 mg of DoN at the dose level 0.75 mg/Kg orally [18]. The SSFMs were suspended in 1 mL saline and administered with the help of J tube. Animals of group II received 25 µL DoN dissolved in 0.9% saline with concentration 6 mg/mL intravenously through tail vein, and the dose was equivalent to 0.75 mg/Kg.

Animals were anaesthetized by intraperitoneal injection of 50 mg/kg ketamine, and 0.5 mL blood was withdrawn through the tail vein at the predetermined time intervals in the heparinized tubes [18]. Subsequently plasma was separated, deproteinized by treating with acetonitrile, and centrifuged. 20 µL of supernatant was injected in the reversed phase C18 column (HiQSil C18 HS (250 × 4.6 mm i.d., particle size 5 µm; KYA Tech Corporation, Japan) and detected by UV detector at 210 nm. The mobile phase contained phosphate buffer pH 7.4, methanol, and acetonitrile (40 : 30 : 30) and flowed at 1.5 mL/min, and at each time point, three rats were tested. Standard calibration curve of DoN was prepared with plasma spiked with known amounts of drug with concentration in the range of 2–10 µg/mL.

2.12.2. Gastroretentive Assessment in Rats.

Microspheres were prepared in the same procedure described previously by adding 50 mg barium sulfate to the 5 mL of glucomannan
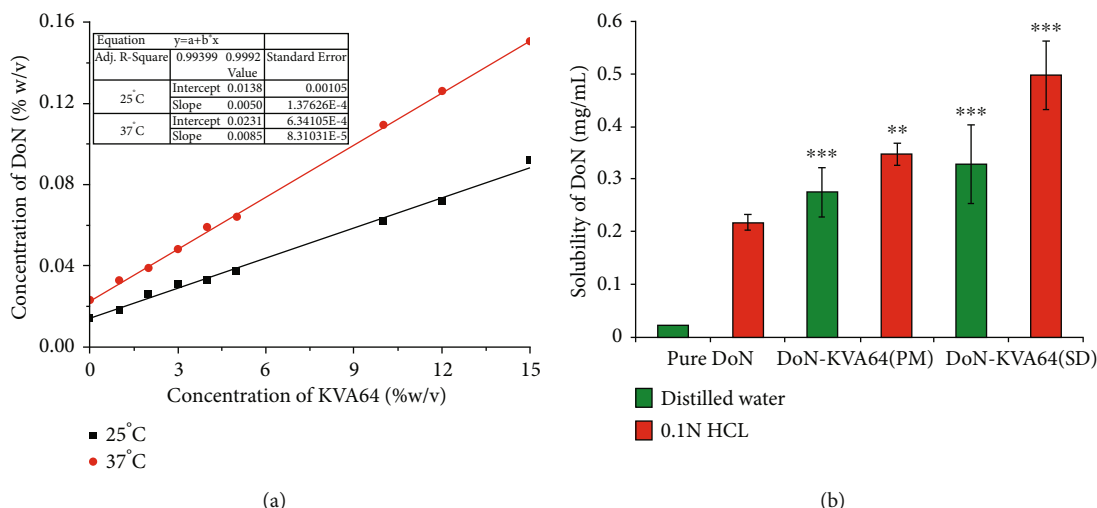
(a)

(b)

FIGURE 1: (a) Phase solubility diagram of DoN in distilled water at 25 and 37°C in the presence of KVA64 and (b) SS data of pure DoN, PM, and SD (mg/mL). $***$ $p < 0.05$ indicates significant differences between the control group and was assessed using the Student t-test.
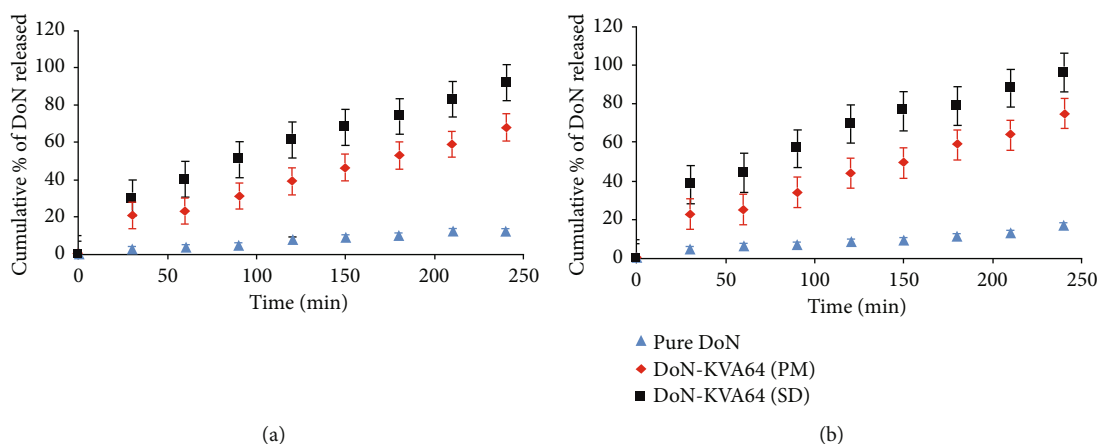

(a)

(b)

FIGURE 2: Dissolution behavior of DoN-KVA64 PM and SD: (a) 0.1 N HCL and (b) distilled water.

solution [19]. Weight of microspheres containing DoN equivalent to 0.75 mg/kg dose was suspended in 1 mL saline and administered per oral route to the rats. X-ray was done, and images were taken at different time points. Three animals were used for the study.

2.13. Stability Study. The prepared DoN microspheres (wrapped in aluminum foil) were stored at 40°C and 75 ± 5% RH for six months as part of a stability investigation. The microspheres were visually evaluated every month for physical changes, DC, PS, and *in vitro* drug release [20].

2.14. Statistical Analysis. The unpaired (two-tailed) t-test was used to compare the data of two groups. The significance threshold was chosen at $p < 0.05$.

3. Result and Discussions

3.1. Outcome from Phase Solubility Data. The phase solubility PS curve displayed linear increase in the solubility of DoN with the increase in KVA64 concentration with corresponding T. The KVA64 concentration was varied from

2.281×10^{-4} to 2.435×10^{-4} mM with 25 and 37°C. The stability constant ($K_{1:1}$) was attained from the complex ranked in the order of 25 and 37°C as DoN (116.14 and 128.05 M⁻¹), which resulted in solubility increase of DoN from 0.171 to 0.433 mM (Figure 1(a)). The equation of the straight line was $y = 0.0.0050x + 01380$, $R^2 = 0.9992$ and $y = 0.0.0085x + 0231$, $R^2 = 0.99399$ at 25 and 37°C, respectively. The curve was A_L type because the slope was less than unity. Mohamed et al. (2021) proven that, this type of curve is obtained when one molecule of DoN complexes with one molecule of the KVA64 as $K_{1:1}$. As the phase solubility curve depicted A_L-type curve, SD was prepared using 1 : 1 ratio of DoN: KVA64 [21].

3.2. SS. The SS of pure DoN in distilled water and 0.1 N HCL at 25°C was found to be 0.0225 and 0.218 mg/mL after 48 h, respectively. There was ~12 and ~14 and ~1.5 and ~2.3 fold improvement in SS of DoN from PM and SD in distilled water and 0.1 N HCL, respectively (Figure 1(b)). The KVA64 is the amorphous carrier which enhances wettability and dispersibility of drug. The surfactant surface properties increase wetting properties by lowering the surface tension

TABLE 2: Micrometric properties of DoN floating microspheres.

Batches	Micrometric properties					EE (%)
	Bulk density	Tap density	Hausner's ratio	Carr's index	Angle of repose	
DF1	0.048 ± 0.02	0.059 ± 0.035	1.229 ± 0.025	0.186 ± 0.035	27.47° ±0.025	88.29 ± 2.89
DF2	0.064 ± 0.15	0.070 ± 0.02	1.093 ± 0.015	0.085 ± 0.065	26.56±0.064	94.93 ± 2.51
DF3	0.119 ± 0.035	0.153 ± 0.035	1.285 ± 0.019	0.222 ± 0.025	31.79±0.034	95.85 ± 3.55
DF4	0.054 ± 0.025	0.080 ± 0.018	1.48 ± 0.025	0.325 ± 0.055	28.81±0.048	91.11 ± 3.76
DF5	0.068 ± 0.044	0.092 ± 0.063	1.35 ± 0.022	0.260 ± 0.0340	39.69±0.06	88.35 ± 3.34
DF6	0.096 ± 0.06	0.137 ± 0.048	1.427 ± 0.36	0.299 ± 0.048	24.70±0.025	92.17 ± 2.11

(a)

0 min   1 h   2 h   4 h

6 h   8 h   10 h   12 h

(b)
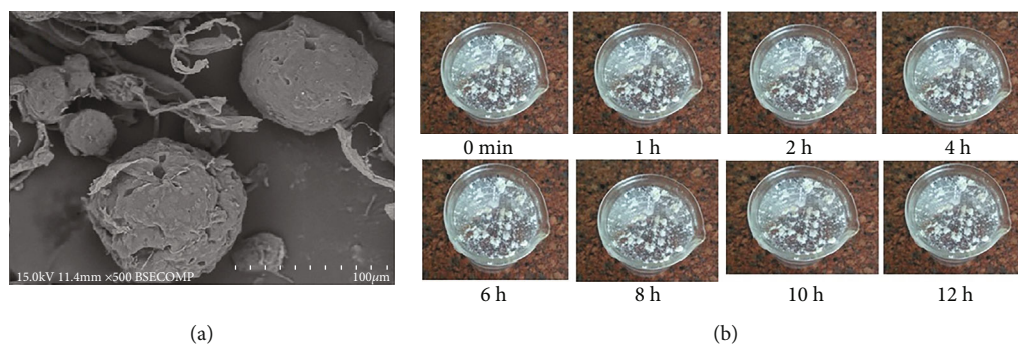
FIGURE 3: (a) Scanning electron micrograph of optimized batch DF2; (b) floating behavior of domperidone floating microsphere (DF2).
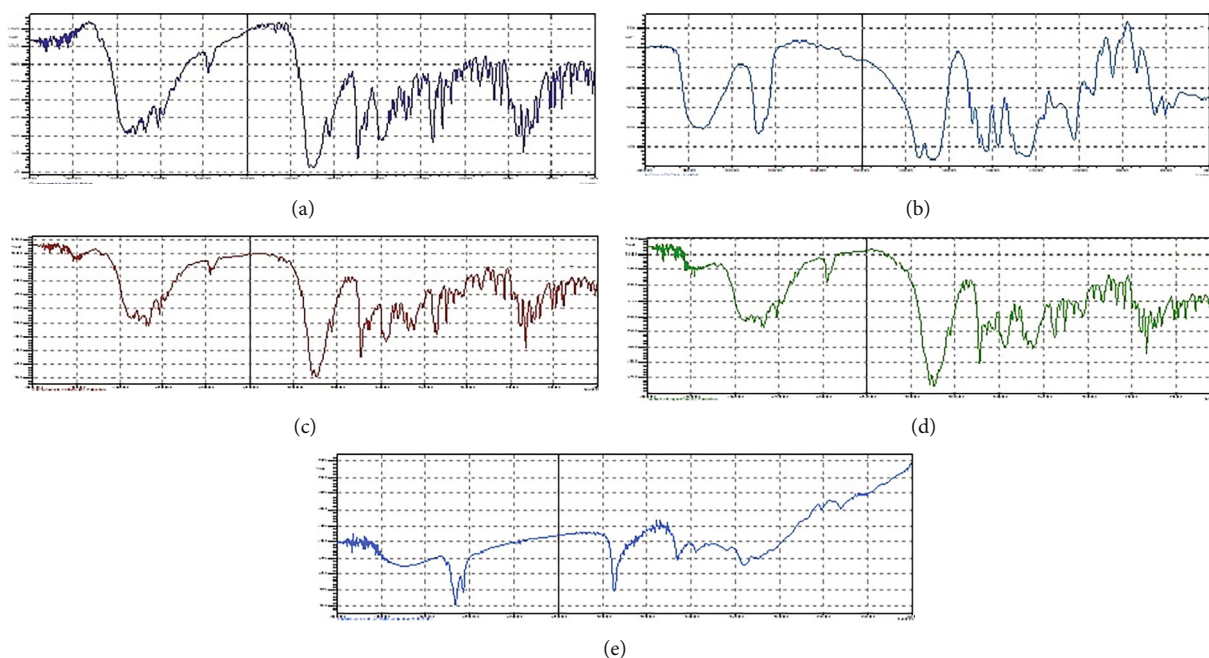

(a)

(b)

(c)

(d)

(e)

FIGURE 4: FI-IR spectrum of (a) pure DoN, (b) KVA64, (c) DoN-KVA64 (PM), (d) DoN-KVA64 (SD), and (e) SSFM-DF2.

of the vehicle utilized, allowing medication molecules to permeate the aqueous environment [22]. Furthermore, the viscosity of KVA64 may affect the solubility of DoN in aqueous environments.

3.3. DC.

The quantity present in the DoN, from prepared SD, ranges from 83.77 to 97.23%, and the material loss with reference to the DoN content was found to be 5.76 to 11.91%

of the material. The moderate material loss was observed with KVA64 because of little cohesive nature and sticky environment in the semisolid state.

3.4. Dissolution of DoN.

The free crystalline DoN release was 12.23 ± 2.16 and 17.12 ± 1.88% in 4 h with distilled water and 0.1 N HCL, respectively, while DoN release from PM was 68.02 ± 4.09 and 75.56 ± 3.32 at the end of 4 h in water
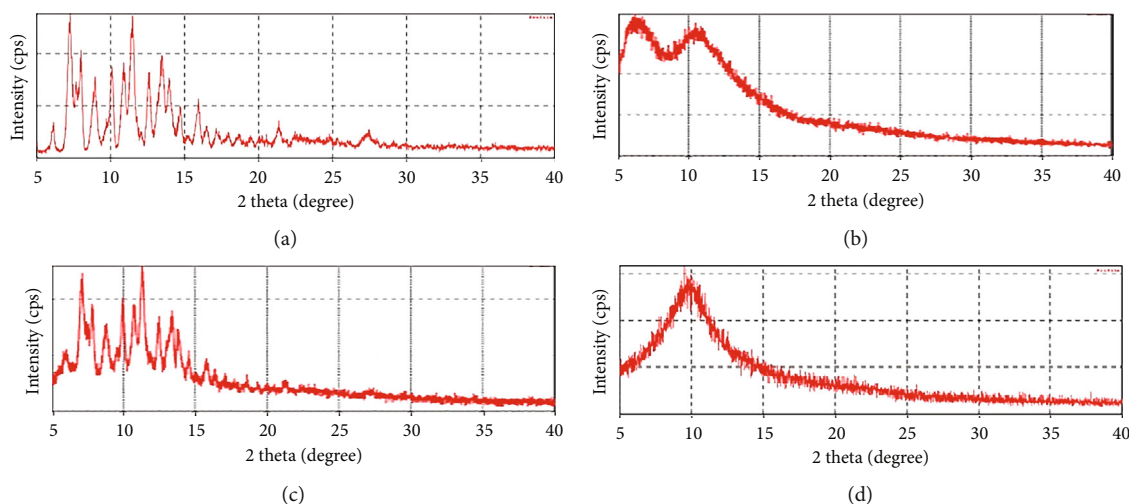
Figure 5: XRD pattern of (a) pure DoN, (b) KVA64, (c) DoN-KVA64 (SD), and (d) SSFM-DF2.

and 0.1 N HCL (Figure 2(a)). Figure 2(b) illustrates rapid initial burst release (30.26 ± 2.06 and $38.71 \pm 3.18\%$ in 30 min) followed by steady release in both distilled water and 0.1 N HCL from prepared SDs with maximum release of 92.11 ± 3.11 and $96.11 \pm 4.4\%$ at the end of 4 h. The controlled dissolution is due to molecular dispersion of DoN in SDs. The reason of the molecular dispersion is that greater surface area of DoN was exposed to the medium. The rapid dissolution was due to DoN molecular dispersion in SD because of the molecule dispersion; DoN surface area was exposed to the medium in higher amounts. Rapid dissolution of KVA64 because of its amorphous and hydrophilic nature resulted in the rapid release of DoN which had transformed into amorphous form upon being dispersed in SD; moreover, SD could dissolve rapidly because of their thermodynamic instability [23].

3.5. EE (%). The percent EE of CRL-MC and CRL-NCs, respectively, was 84.12 ± 0.33 and 83.61 ± 0.80 percent (Table 2). CRL lipophilicity (log P = 3.8) can be attributed to these low percent EE values, allowing it to be efficiently integrated into PVP/SDS dual carriers in the prepared formulations. According to Alqahtani et al., a lipophilic drug might enhance EE by employing lipid as an encapsulating carrier [24].

3.6. Micromeritics. The mean PS of DoN floating microspheres was in the range of 16.20 ± 0.036 to 25.19 ± 0.041 μm. The PS was found dependent on the concentration of KGM and ratio of KGM to cross-linker (glutaraldehyde). The PS was found to be larger for batches DF3 and DF6 because viscosity of 2% w/v KGM used in their formulation was appreciably high, which could have affected appropriate diffusion of glutaraldehyde in KGM phase for cross-linking. Additionally, amount of cross-linker might perhaps be insufficient for the stated amount of KGM to form dense network. The rank order for particle size was DF1< DF2 < DF3. At low level of KGM, there was better cross-linking as a result of which dense particles with small size were formed.
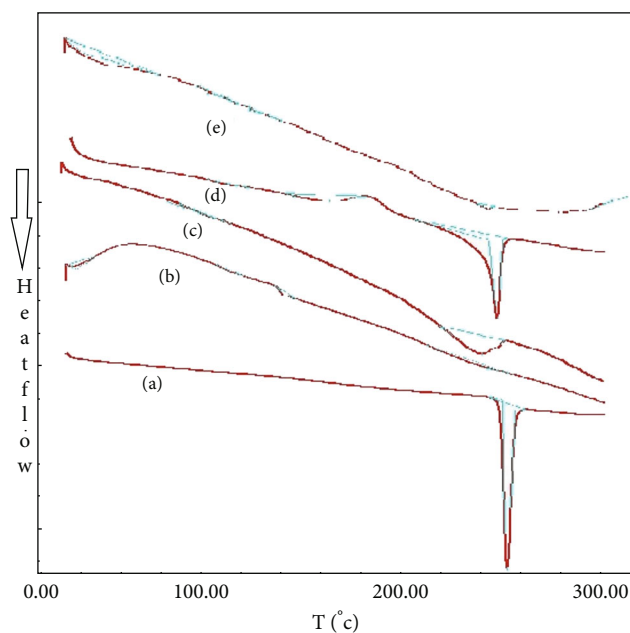

Figure 6: DSC thermogram of (a) pure DoN, (b) KVA64, (c) DoN-KVA64 (PM), (d) DoN-KVA64 (SD), and (e) SSFM-DF2.

3.7. Morphology. In Figure 3(a), the microspheres were spherical with nearly smooth surface. From the SEM, cross-linked surface was evident. There were few pores on the surface which could be due to diffusion of hydrophilic KVA64 from the microspheres during drug loading and cross-linking process.

3.8. Buoyancy In Vitro. The microspheres became buoyant immediately and remained floating for more than 12 h. First, the low density of the microspheres formed from glucomannan held them on the surface. Second, quick and high polymer hydration resulted in a quick volume enlargement of the microspheres, which served to lower the density and
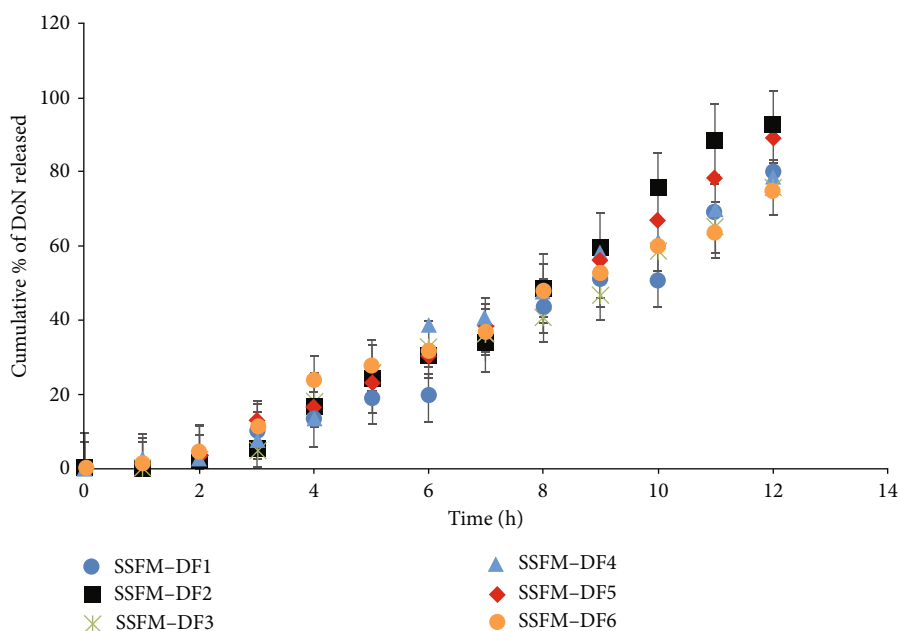
Figure 7: *In vitro* DoN released from various SSFMs.

Table 3: Treatment of *in vitro* drug release data with different kinetic equations.

Batches	Mathematical model (r^2)					
	Zero order	First order	Hixson-Crowell	Higuchi plot	Korsmeyer-Peppas	Release exponents
DF1	0.985 ± 0.048	0.928 ± 0.087	0.987 ± 0.089	0.952 ± 0.043	0.895 ± 0.043	1.201 ± 0.192
DF2	0.994 ± 0.056	0.931 ± 0.087	0.991 ± 0.051	0.951 ± 0.047	0.861 ± 0.033	1.567 ± 0.091
DF3	0.992 ± 0.091	0.903 ± 0.076	0.972 ± 0.043	0.973 ± 0.068	0.842 ± 0.081	1.786 ± 0.213
DF4	0.992 ± 0.055	0.913 ± 0.076	0.982 ± 0.054	0.973 ± 0.032	0.881 ± 0.018	1.887 ± 0.134
DF5	0.990 ± 0.061	0.913 ± 0.064	0.992 ± 0.067	0.960 ± 0.078	0.907 ± 0.043	1.524 ± 0.157
DF6	0.996 ± 0.075	0.876 ± 0.092	0.973 ± 0.067	0.983 ± 0.078	0.916 ± 0.032	1.096 ± 0.155

significantly improve the buoyancy of the microspheres [25]. In low pH condition, cross-linked KGM microspheres remained stable and therefore kept floating throughout the 12-h study (Figure 3(b)). The strength of beta chain in glycosidic linkage of glucomannan might have been responsible for stability of microspheres in the low pH condition. Glutaraldehyde synthesis of cross-linked konjac-glucomannan and kappa carrageenan films).

3.9. Solid-State Characterization of DPASD by FTIR, DSC, and XRD

3.9.1. FTIR. FT-IR spectra of DoN and physical mixture of DoN and Kollidon VA 64 were used to examine likely molecular interactions between DoN and KVA64 in the solid state and to detect the change in characteristics of DoN if any, in ASD. Characteristic IR peaks of DoN were observed at 3122.54, 3024.18, 2923.88, 1716.53, 1670.24, and 1622.02 cm^{-1} due to NH group, aromatic CH stretching, aliphatic CH group stretching, C=O stretching, NH diffraction, and C-H diffraction (scissoring), respectively (Figure 4). All the characteristic peaks were retained in the

physical mixture of DoN and KVA64. The peaks attributed to DoN were unaltered in the FTIR of SD also, denying any possible chemical interaction between DoN and KVA64 in solid dispersion [26].

FTIR of domperidone shows characteristic peaks at 3122.54 cm^{-1} due to NH group stretching imide, 3024.18 cm^{-1} due to aromatic C-H stretching, 2923.88 cm^{-1} due to aliphatic C-H group stretching, 1716.534 and 1695.31 cm^{-1} due to C=O stretching, 1670.24 and 1622.02 cm^{-1} due to NH diffraction, and 1456.16 cm^{-1} due to C-H diffraction (scissoring).

3.9.2. XRD. X-ray diffraction (XRD) analysis of DoN exhibited distinctive diffraction peaks at $2\theta = 14.49°$, $18.36°$, $19.5°$, $20°$, $21°$, and $22.8°$ (Figure 5) which confirms crystalline nature of the drug. These characteristics peaks were retained in the physical mixture implicating no change in the crystal behavior of DoN. However, the diffraction pattern for solid dispersion depicted peaks at $2\theta = 14.55°$, $15.02°$, $15.64°$, $18.45°$, $19.74°$, $19.98°$, $22°$, and $22.65°$ which were different from that of DoN demonstrating change in crystal structure. There is no sharp peaks in KVA64 confirming its
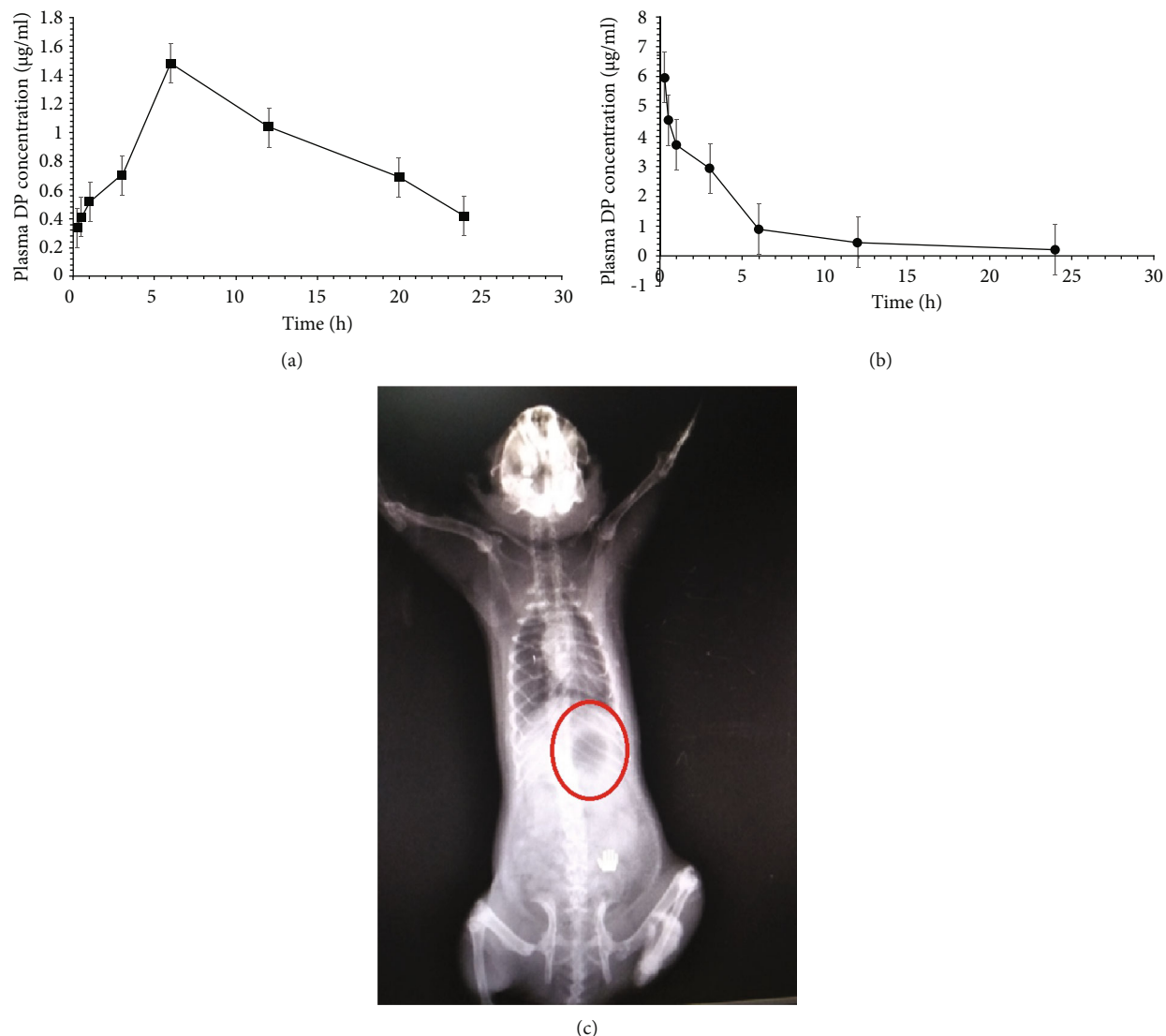
(a)

(b)

(c)

FIGURE 8: Plasma DoN concentration at (a) oral route, (b) intravenous of administration, and (c) 12 h after dosage, radiographic X-ray pictures of the formulation in the rat gastrointestinal region.

TABLE 4: Pharmacokinetic parameters of DoN after i.v. and oral floating microspheres administration.

S. no	Parameters	Intravenous	Oral
1	C_{max} (μg/mL)	5.99 ± 0.562†	1.48 ± 0.54234
2	C0 (μg/mL; extrapolated)	7.88 ± 0.527	—
3	T_{max} (h)	—	6
4	AUC $_{0-24}$ (μg/mL∗h)	25.92 ± 6.481	21.55 ± 4.65
5	$t^{1/2}$ (h)	9.07 ± 0.771	10.47 ± 0.6746
6	MRT (h)	8.42 ± 1.269	17.36 ± 1.4386

†: nonextrapolated.

amorphous nature (Figure 5(b)). Reduction in intensity of characteristic peaks was observed in physical mixture, which might be because of partial masking of peaks of drug [27]. Change in the position of peaks of the drug and appearance of the new peaks in the solid dispersion indicates change in the crystalline nature of the drug. Sharp intense peaks of drug was completely missing in microspheres, indicating entrapment of DoN in the microspheres.

3.9.3. DSC. The DSC thermogram of DoN exhibited a characteristic, sharp endothermic peak at 253.2°C which is associated with the melting point of the drug and indicates the crystalline nature (Figure 6(a)). The peak is slightly broadened in the solid dispersion due to the reduction in crystalline of DoN. The broad endothermic peak at 244.68°C in the physical mixture of DoN and Kollidon corresponds to the melting of DoN. Broadening of peak and reduction in temperature indicate decrease in crystallinity [28]. Broadened endothermic peak at reduced temperature of 25°C confirms decrease in crystallinity of DoN. There was a small endothermic peak of the drug in microsphere at reduced T of 246.63°C indicating decreased crystallinity and encapsulation in the microspheres.

TABLE 5: Various stability parameters of CRL-NCs.

Evaluations	0 month	1 month	3 month	6 month
DC * (%)	96.66 ± 0.32	94.94 ± 1.34	92.15 ± 1.79	89.95 ± 2.66
PS * (μm)	163.71 ± 2.26	167.38 ± 3.98	168.11 ± 4.45	170.88 ± 4.11
EE (%) *	94.93 ± 2.51	91.12 ± 3.23	79.44 ± 2.85	76.54 ± 4.19
In vitro release (after 12 h)*	92.62 ± 2.43	90.21 ± 4.16	87.33 ± 5.32	84.71 ± 5.41

*Each value expressed as mean, ($n = 3$; ± SD).

3.10. In Vitro Drug Release. The cumulative % drug release of all SSFM-DF1 to SSFM-DF6 was in range of 73.59 ± 0.41 to 92.62 ± 2.43% in 12 h (Figure 7). Rate of drug release was slower from DF1 as compared to DF2 because the particles were more strongly cross-linked; thus, there was restricted diffusion of drug. Microparticles prepared from high level of KGM (DF3 and DF6) also produced slow dissolution rates. In case of DF3 and DF6, the initial drug release rate was controlled by cross-linking, while with the slumping cross-link strength as the time passed, the viscous gel network due to high level of KGM played predominant role in controlling the drug release rate during later time points.

Formulation DF2 gave maximum drug release (92.62 ± 2.43%) in 12 h (Table 3). Maximum linearity was observed for zero order ($R^2 = 0.994$), while slope of Korsmeyer-Peppas equation was found 1.567. Slope greater than one indicates super case II that is drug release by diffusion and chain relaxation [29]. Drug release by chain relaxation often happens in cross-linked matrices where cross-linking strength declines with time.

3.11. In Vivo Bioavailability Testing. Figures 8(a) and 8(b) show the mean plasma drug concentration time curve of DoN following oral, and i.v. administration of DoN-loaded SSFM, respectively. Table 4 lists the noncompartment pharmacokinetic parameters determined using the software PKSolver. After oral administration of microspheres, the maximal blood concentration was reached at 6 h, and a consistent level of drug was continued for another 12 h. The constant level of DoN was due to prolonged retention of microspheres in the stomach and uniform and prolonged release of the drug in the stomach.

The absolute bioavailability of the DoN from floating microspheres was 83 ± 0.579%, which was significantly higher than its reported oral bioavailability of 13 to 17% [30]. The improvement in bioavailability from floating microspheres may be attributed to the improvement in solubility of DoN by solid dispersion and gastroretention of the microspheres in the environment where solubility was good. The mean residence time of drug from microspheres (17.36 ± 1.4 h) and $t_{1/2}$ (10.47 ± 0.6 h) were significantly greater ($p < 0.05$) than obtained after i.v. administration (MRT = 8.42 ± 1.2 h; $t_{1/2}$ = 9.07 ± 0.7 h).

3.12. Radiographic Study in Rats. The floating capability of SSFM was tested in simulated gastric fluid for enhanced stomach residence. KGM: SD (1.5 : 67.5 percent w/w) was used to make DF2, and DF2 with high *in vitro* buoyancy

was chosen for further testing using the radiological approach. The gastroretentive feature of microspheres is evident in X-ray images collected at 0 and 12 h for the buoyancy investigation (Figure 8(c)), stressing a large gastric residency period for optimal drug release and absorption at stomach fluid due to the porous structure of SSFMs [31].

3.13. Stability Studies. The CRL-NCs was maintained for further characterization and stability testing. According to the data in Table 5, the SSFM remained stable for six months at 45 ± 0.5°C and 60% RH. Only a minor increase in PS (170.88 ± 4.11 μm) was noticed after six month storage. In another hand, very little impact on DC, % EE, and cumulative *in vitro* DoN release was observed after storage such as 89.95 ± 2.66%, 76.54 ± 4.19%, 87.34 ± 3.11%, respectively. This outcome suggests that, when stored at RT, CRL-NCs have a good physical stability [32].

4. Conclusion

High degree of improvement in solubility of SD could be achieved for DoN using KVA64 in both distilled water and 0.1 N HCL which was then loaded successfully in floating microsphere containing KGM. It was then prepared by emulsion cross-linking method with the entrapment efficiency as high as 94.93 ± 2.51% from the present study, and it was found that glucomannan microspheres had the inherent property to float without the aid of any floating agent. The improvement in *in vivo* bioavailability from SSFM-DF2 might be attributed to the improvement in solubility of DoN by SD and gastroretention of the microspheres where solubility was good. Therefore, KGM can serve as a potential polymeric carrier for formulation of floating microsphere by very simple reproducible and scalable technique as achieved in the present investigation.

Data Availability

The original contributions presented in the study are included in the article; further inquiries can be directed to the corresponding author.

Conflicts of Interest

The authors declare that they have no conflicts of interest.

Acknowledgments

References

[1] K. T. Savjani, A. K. Gajjar, and J. K. Savjani, "Drug solubility: importance and enhancement techniques," *ISRN Pharmacology*, vol. 2012, Article ID 195727, 10 pages, 2012.

[2] S. Verma, A. Rawat, M. Kaul, and S. Saini, "Solid dispersion: a strategy for solubility enhancement," *Inter JIPBS Pharmacy Tech*, vol. 2, no. 4, pp. 482–494, 2015.

[3] V. P. Bharti, V. R. Attal, A. V. Munde, A. S. Birajdar, and S. Bais, "Strategies to enhance solubility and dissolution of a poorly water soluble drug," *Journal of Innovations in Pharmaceuticals and Biological Sciences*, vol. 2, no. 4, pp. 482–494, 2015.

[4] P. Paulsamym, K. Venkatesan, J. M. Muthu Mohamed et al., "Empowerment of primary healthcare providers on the prevention and management of dental or oral health issues among postchemotherapy patients in pandemic," *Journal of Healthcare Engineering*, vol. 2022, Article ID 9087776, 9 pages, 2022.

[5] H. Suzuki, K. Yakushiji, S. Matsunaga et al., "Amorphous solid dispersion of meloxicam enhanced oral absorption in rats with impaired gastric motility," *Journal of Pharmaceutical Sciences*, vol. 107, no. 1, pp. 446–452, 2018.

[6] F. S. Razavi, M. Kouchak, F. Feizoleslam, and M. Veysi, "An overview on floating drug delivery systems (FDDS); conventional and new approaches for preparation and *in vitro–in vivo* evaluation," *FABAD Journal of Pharmaceutical Sciences*, vol. 46, no. 3, pp. 345–362, 2021.

[7] K. Thakar, G. Joshi, and K. K. Sawant, "Bioavailability enhancement of baclofen by gastroretentive floating formulation: statistical optimization, in *vitro* and *in* vivo pharmacokinetic studies," *Drug Development and Industrial Pharmacy*, vol. 39, no. 6, pp. 880–888, 2013.

[8] J. Apiwongngam, W. Limwikrant, A. Jintapattanakit, and M. Jaturanpinyo, "Enhanced supersaturation of chlortetracycline hydrochloride by amorphous solid dispersion," *Journal of Drug Delivery Science and Technology*, vol. 47, pp. 417–426, 2018.

[9] T. Charoenying, P. Patrojanasophon, T. Ngawhirunpat, T. Rojanarata, P. Akkaramongkolporn, and P. Opanasopit, "Design and optimization of 3D-printed gastroretentive floating devices by central composite design," *AAPS PharmSciTech*, vol. 22, no. 5, p. 197, 2021.

[10] T. Higuchi and K. A. Connors, "Phase solubility techniques," *Advances in Analytical Chemistry*, vol. 4, pp. 117–119, 1965.

[11] M. M. Jamal Moideen, A. Alqahtani, K. Venkatesan et al., "Application of the Box-Behnken design for the production of soluble curcumin: skimmed milk powder inclusion complex for improving the treatment of colorectal cancer," *Food Science & Nutrition*, vol. 8, no. 12, pp. 6643–6659, 2020.

[12] M. J. Muthu, K. Kavitha, K. S. Chitra, and S. Nandhineeswari, "Soluble curcumin prepared by solid dispersion using four different carriers: phase solubility, molecular modelling and physicochemical characterization," *Tropical Journal of Pharmaceutical Research*, vol. 18, no. 8, pp. 1581–1588, 2019.

[13] J. M. M. Mohamed, A. Alqahtani, B. A. Khan et al., "Preparation of soluble complex of curcumin for the potential antagonistic effects on human colorectal adenocarcinoma cells," *Pharmaceuticals*, vol. 14, no. 9, p. 939, 2021.

[14] D. R. Getts, R. L. Terry, M. T. Getts et al., "Therapeutic inflammatory monocyte modulation using immune-modifying microparticles," *Science Translational Medicine*, vol. 6, no. 219, p. 219ra7, 2014.

[15] C. Thapa and R. Chaudhary, "Formulation and in-vitro evaluation of sustained release matrix tablets of domperidone," *Journal of Universal College of Medical Sciences*, vol. 8, pp. 40–45, 2021.

[16] A. R. Dhole, P. D. Gaikwad, V. H. Bankar, and S. P. Pawar, "A review on floating multiparticulate drug delivery system: a novel approach to gastric retention," *International Journal of Pharmaceutical Sciences Review and Research*, vol. 2, pp. 205–211, 2011.

[17] J. M. Mohamed, A. Alqahtani, F. Ahmad, V. Krishnaraju, and K. Kalpana, "Pectin co-functionalized dual layered solid lipid nanoparticle made by soluble curcumin for the targeted potential treatment of colorectal cancer," *Carbohydrate Polymers*, vol. 252, p. 117180, 2020.

[18] U. K. Mandal, B. Chatterjee, and F. G. Senjoti, "Gastro-retentive drug delivery systems and their *in vivo* success: a recent update," *Asian Journal of Pharmaceutical Sciences*, vol. 11, no. 5, pp. 575–584, 2016.

[19] F. Schneider, M. Koziolek, and W. Weitschies, "*In vitro* and *in vivo* test methods for the evaluation of gastroretentive dosage forms," *Pharmaceutics*, vol. 11, no. 8, p. 416, 2019.

[20] J. M. M. Mohamed, A. Alqahtani, A. al Fatease et al., "Human hair keratin composite scaffold: characterisation and biocompatibility study on NIH 3T3 fibroblast cells," *Pharmaceuticals*, vol. 14, no. 8, p. 781, 2021.

[21] J. M. Mohamed, K. Kavitha, K. Ruckmani, and S. Shanmuganathan, "Skimmed milk powder and pectin decorated solid lipid nanoparticle containing soluble curcumin used for the treatment of colorectal cancer," *Journal of Food Process Engineering*, vol. 43, no. 3, pp. 1–15, 2020.

[22] S. Parvate, P. Dixit, and S. Chattopadhyay, "Superhydrophobic surfaces: insights from theory and experiment," *The Journal of Physical Chemistry B*, vol. 124, no. 8, pp. 1323–1360, 2020.

[23] A. K. Sav, H. Desai, M. Tarique, and P. Amin, "Solubility and dissolution rate enhancement of curcumin using Kollidon VA64 by solid dispersion technique," *International Journal of Pharm Tech Research*, vol. 4, no. 3, pp. 1055–1064, 2012.

[24] A. Alqahtani, B. Raut, S. Khan et al., "The unique carboxymethyl fenugreek gum gel loaded itraconazole self-emulsifying nanovesicles for topical onychomycosis treatment," *Polymers*, vol. 14, no. 2, p. 325, 2022.

[25] A. Y. Kaushik, A. K. Tiwari, and A. Gaur, "Role of excipients and polymeric advancements in preparation of floating drug delivery systems," *International Journal of Pharmaceutical Investigation*, vol. 5, no. 1, pp. 1–12, 2015.

[26] M. Nagpal, L. Kaur, J. Chander, and P. Sharma, "Dissolution enhancement of domperidone fast disintegrating tablet using modified locust bean gum by solid dispersion technique," *Journal of Pharmaceutical Technology, Research and Management*, vol. 4, no. 1, pp. 1–11, 2016.

[27] A. E. Aboutaleb, S. I. Abdel-Rahman, M. O. Ahmed, and M. A. Younis, "Improvement of domperidone solubility and dissolution rate by dispersion in various hydrophilic carriers," *Journal of Applied Pharmaceutical Science*, vol. 6, no. 7, pp. 133–139, 2016.

[28] J. M. M. Mohamed, F. Ahmad, A. Alqahtani, T. Alqahtani, V. K. Raju, and M. Anusuya, "Studies on preparation and evaluation of soluble 1:1 stoichiometric curcumin complex for colorectal cancer treatment," *Trends in Sciences*, vol. 18, no. 24, p. 1403, 2021.

[29] J. M. M. Mohamed, A. Alqahtani, T. V. A. Kumar et al., "Superfast synthesis of stabilized silver nanoparticles using aqueous *Allium sativum* (garlic) extract and isoniazid hydrazide conjugates: molecular docking and *in-vitro* characterizations," *Molecules*, vol. 27, no. 1, p. 110, 2022.

[30] G. M. Zayed, S. A. Rasoul, M. A. Ibrahim, M. S. Saddik, and D. H. Alshora, "*In vitro* and *in vivo* characterization of domperidone-loaded fast dissolving buccal films," *Saudi Pharmaceutical Journal*, vol. 28, no. 3, pp. 266–273, 2020.

[31] S. T. Ndlovu, N. Ullah, S. Khan et al., "Domperidone nanocrystals with boosted oral bioavailability: fabrication, evaluation and molecular insight into the polymer-domperidone nanocrystal interaction," *Drug Delivery and Translational Research*, vol. 9, no. 1, pp. 284–297, 2019.

[32] J. M. M. Mohamed, A. Alqahtani, F. Ahmad, V. Krishnaraju, and K. Kalpana, "Stoichiometrically governed curcumin solid dispersion and its cytotoxic evaluation on colorectal adenocarcinoma cells," *Drug Design, Development and Therapy*, vol. 14, pp. 4639–4658, 2020.